Very low-grade metamorphism in the para-autochtonous sedimentary cover of the Pelvoux massif (Western Alps, France)

Sébastien Potel, Ghislain Trullenque

Swiss J Geosci (2012) 105:235–247
DOI 10.1007/s00015-012-0102-8

Very low-grade metamorphism in the para-autochtonous sedimentary cover of the Pelvoux massif (Western Alps, France)

Sébastien Potel · Ghislain Trullenque

Received: 14 November 2011 / Accepted: 14 May 2012 / Published online: 19 August 2012

Abstract The metamorphic grade from the para-autochtonous cover of the Pelvoux massif (PM, western Alp, France) was investigated in Priabonian metamarls, through mineral assemblages, simultaneous measurements of illite and chlorite "crystallinity", K-white mica *b* cell dimension and K-white mica polytypes content. Kübler (KI) and Árkai (ÁI) indexes display values characteristic for uppermost diagenetic to low anchizonal conditions. These results are supported by the incomplete transformation of K-white mica polytypes from $1M_d$ and $2M_1$ and are in line with the not annealed status of zircon fission tracks in the southeast zone of the Pelvoux massif (Seward et al. 1999). Our findings differ from previous results, which suggested epizonal conditions at several places in the northern part of our field area, but are coherent with the temperature estimation suggested by the mineral assemblage described in the literature. These results are further supported by temperature values deduced from fluid inclusion investigations. A small decrease of KI and ÁI values is observed within the basal decollement level of the Priabonian cover, when going from the least deformed zones to the most deformed ones. K-white mica *b* cell dimensions in micas of the area are in the range 9.000–9.040 Å, which corresponds to an inferred geothermal gradient of 25–35 °C/km, similar to the values found further north in the Dauphinois domain (Ceriani et al. 2003). This indicates a long steady state heat flow corresponding to a long term metamorphic event like in the eastern Alps.

Keywords Illite crystallinity · Very low-grade metamorphism · Western Alps · External crystalline massif

Editorial handling: Rafael Ferreiro Mählmann and Edwin Gnos.

Present Address:
S. Potel (✉)
Institut Polytechnique LaSalle Beauvais-Equipe B2R,
19 rue Pierre Waguet, BP 30313, 60026 Beauvais Cedex, France
e-mail: sebastien.potel@lasalle-beauvais.fr

S. Potel
Insitut für Geowissenschaften und Lithosphärenforschung,
Universität Giessen, Giessen, Germany

Present Address:
G. Trullenque
Institut für Geowissenschaften, Geologie, Universität Freiburg,
Albertstrasse 23b, Freiburg, Germany

G. Trullenque
Institute of Geology and Paleontology, University of Basel,
Basel, Switzerland

1 Introduction

In the western Alps, the illite "crystallinity" method has been used in order to differentiate the anchizone from diagenesis and epizone domains according to Kübler (1968). The general trend of the metamorphic grade, increasing from W to E, from diagenesis to epizone, is perturbed by tectonic duplexes and the influence of crystalline basement (Desmons et al. 1999).

In the northern part of the Pelvoux massif, Ceriani et al. (2003) studied the low-grade metamorphism in the region of the Frontal Penninic units (FPU) of the Western Alps between the Arc and Isère Valleys (Fig. 1a, b). The results of the study allowed relating the metamorphism to the different stages of deformation.

Previous metamorphic studies described south of the Pelvoux massif a laumontite–prehnite–pumpellyite subfacies (zeolite facies) in the "grès de Champsaur" formation,

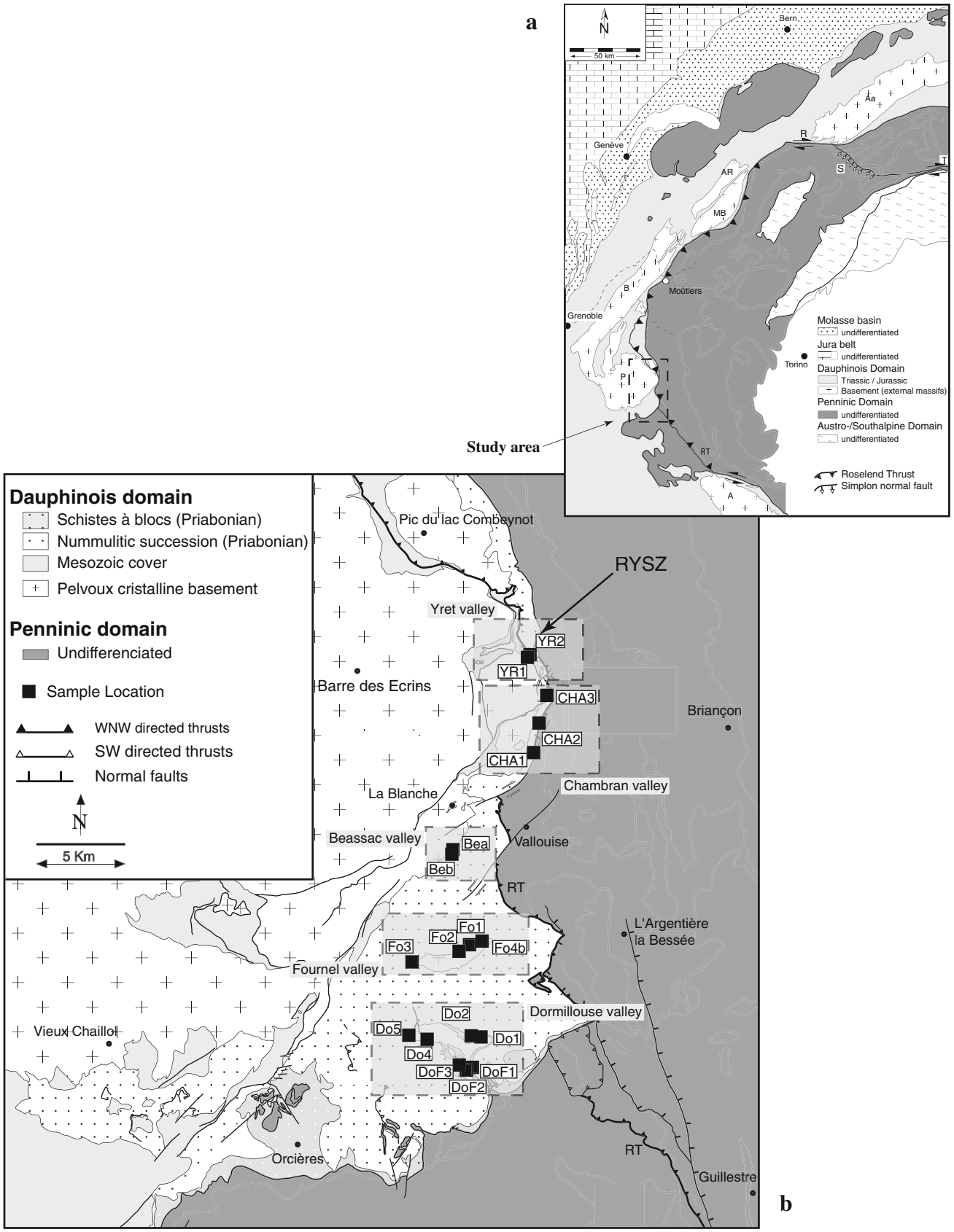
a
N
50 km
Bern
Genève
Aa
R
S
T
AR
MB
B
Moûtiers
Grenoble
P
RT
A
Torino
Molasse basin
undifferentiated
Jura belt
undifferentiated
Dauphinois Domain
Triassic / Jurassic
Basement (external massifs)
Penninic Domain
undifferentiated
Austro-/Southalpine Domain
undifferentiated
Roselend Thrust
Simplon normal fault
Study area
Dauphinois domain
Schistes à blocs (Priabonian)
Nummulitic succession (Priabonian)
Mesozoic cover
Pelvoux cristalline basement
Penninic domain
Undifferenciated
Sample Location
WNW directed thrusts
SW directed thrusts
Normal faults
N
5 Km
Pic du lac Combeynot
RYSZ
Yret valley
YR2
YR1
Barre des Ecrins
CHA3
CHA2
CHA1
Briançon
La Blanche
Chambran valley
Beassac valley
Bea
Beb
Vallouise
RT
Fo1
Fo2
Fo3
Fo4b
L'Argentière
la Bessée
Fournel valley
Do2
Dormillouse valley
Do5
Do1
Vieux Chaillol
Do4
DoF3
DoF1
DoF2
Orcières
RT
Guillestre
b

◀ **Fig. 1** **a** Simplified geological overview of the arc of the western Alps (*A* Argentera massif, *CM* Combeynot massif, *MB* Mont Blanc massif, *P* Pelvoux massif, *R* Rhone-Simplon line, *T* Tonale line); after Ferreiro Mählmann (1996), Ceriani et al. (2001) and Ravenne et al. (1987, 2004). **b** Tectonic map along the eastern rim of the Pelvoux massif compiled from (1) geological maps BRGM (1/50,000): La Grave, Briançon, St Christophe en Oisans, Guillestre, Orcières and Embrun and (2) Tricart (1986). Points Yr, Fo, Be, Cha, Do and DoF refer to samples studied, collected at the eastern rim of the Pelvoux massif, in the Yret, Fournel, Beassac, Chambran, Dormillouse and Dormillouse-Fangeas valleys, respectively. *RT* Roselend Thrust, *RYSZ* Rocher de l'Yret shear zone

with rock-forming laumontite (Aprahamian 1988) and pumpellyite–prehnite in veins (Waibel 1990). On the metamorphic map of the Alps (Frey et al. 1999) and the map of metamorphic structure of the Alps (Oberhänsli et al. 2004) the sub-greenschist facies (epizone) is found in the tiny basement of Fournel and Dormillouse valleys (ref. Fig. 1b).

The aim of this contribution is to present the results of a study on metamorphic grade in the southern footwall of the Penninic Basal Contact (PBC, Ceriani et al. 2001), within the Dauphinois cover of the southeastern rim of the Pelvoux massif, and to compare the results with those from Ceriani et al. (2003). The metamorphic grade was investigated in the globigerina metamarl level and in the Mesozoic cover by mineral assemblages, simultaneous measurements of illite and chlorite "crystallinity" using the KI- and ÁI-methods, K-white mica *b* cell dimension and K-white mica polytypes content. Within the Rocher de l'Yret shear zone (RYSZ, Fig. 1), results are completed by a fluid inclusion study. Quartz precipitates found along the strike slip fault planes dissecting the uppermost basement units from the RYSZ were analysed. All the methods were used for a better P–T estimate to get a higher precision on the metamorphic evolution in this region and to conclude better with some geodynamic implications. The results of this metamorphic study are compared to those from Ceriani et al. (2003) north of the Pelvoux massif, to the FT data available in the region (Seward et al. 1999; Fügenschuh and Schmid 2003) and previous studies describing mineral assemblage in the "grès de Champsaur" (Aprahamian 1988; Waibel 1990).

2 Regional geology

The Dauphinois domain is part of the European margin and composed of Variscan basement carrying a thick Permian to Tertiary sedimentary cover. During Mesozoic rifting, the eastern margin of the European plate was substantially thinned. Formation of major tilted crustal blocks allowed for the deposition of thick Mesozoic sedimentary series in asymmetric half grabens intensively described in literature (Tricart et al. 1988; Davies 1982; Gillcrist et al. 1987; Butler 1989; Coward et al. 1991; Huyghe and Mugnier 1995; Lazarre et al. 1996; Sue et al. 1997).

Mesozoic strata are discordantly overlain by a conglomerate formation (Gupta 1997), followed by the classical "Priabonian trilogy" (Ravenne et al. 1987; Apps et al. 2004), which comprises, from base to top: (1) shallow water nummulitic limestone of variable thickness (0–50 m), (2) hemipelagic globigerina marls (0–50 m), and (3) the "grès de Champsaur" formation, a regular alternance of turbiditic sandstones and shales (Perriaux and Uselle 1968; Waibel 1990), whose thickness varies from 700 to 1,200 m. In some areas immediately south of the Pelvoux massif, the siliciclastic deposits contain up to 50 % of volcanic detritus (Debrand-Passard et al. 1984; Bürgisser 1998).

Locally, three Alpine deformation phases (D_1, D_2 and D_3) can be recognized (Trullenque 2005). D_1, first phase of deformation that affected the Dauphinois units corresponds to the third phase of deformation described by Ceriani et al. 2001, i.e. Oligocene to lower Miocene out of sequence thrusting along the Roselend thrust (RT). It is the major deformation phase encountered in the investigated area since it is related to the thrusting along the RT (Ceriani et al. 2001). D_1 deformation structures constantly show WNW-directed kinematic indicators measured directly along tectonic contacts, i.e. consistent with activity along the RT.

The second D_2 deformation phase recorded within the investigated area results in SW-directed movements that overprint the top-WNW D_1 deformation features and which are missing N of the Pelvoux massif. Trullenque (2005) proposed that the D_2 top-SW deformation phase is linked to the formation of the Apeninnes chain, as a consequence of the opening of the Thyrenian basin during Langhian times.

D_3 structures, normal faults related to the Durance fault system (High Durance Faulted Zone, Tricart 2004) are the latest deformation features found in the investigated area. These normal faults are notably responsible for a strong geothermal gradient and seismicity recorded along the Durance valley. The timing of the onset of normal faulting, also recorded north of Pelvoux, remains a matter of debate (see Fügenschuh et al. 1999; Fügenschuh and Schmid 2003; Tricart et al. 2001). However, in this region, fission track data on zircon (Seward et al. 1999) reveal that maximum temperatures were well below greenschist facies conditions. Seward et al. (1999) interpreted the heating event as being due to the emplacement of internal thrust sheets, which thin out westwards.

3 Materials and methods

In marine pelites and carbonates, no diagnostic minerals and mineral assemblages form at conditions of very

low-grade field. In these rocks, the transitions from non-metamorphic to very low-grade and from very low-grade to low-grade metamorphic domains take place through the diagenetic zone, the anchizone and the epizone, each zone being characterized by specific values of the illite Kübler Index (KI; Árkai et al. 2003). The illite "crystallinity" (IC or KI; Kübler 1964) is defined as the full width at half maximum of the first illite basal reflection in XRD patterns (Frey 1987; Guggenheim et al. 2002). Guggenheim et al. (2002) recommended that the use of a "crystallinity index" should be avoided, although it may be placed within quotation marks when referring in a limited way to previously referenced work. They also recommended to refer to an index by relating it to the author describing the procedures necessary to define the value, regardless of what the index may actually be describing. Therefore, we will refer for K-white mica to the illite "crystallinity" for raw data and to KI after calibration against Kübler's scale.

Illite "crystallinity" is considered to be a function of crystallite thickness, the number of lattice defects (Merriman et al. 1990). Temperature is thought to be the main factor controlling the illite "crystallinity", but other parameters like lithology, time, tectonic stress and fluid/rock ratio may probably have important effect (see Frey 1987). Árkai (1991) and Árkai et al. (1995) proposed a similar index the chlorite "crystallinity" (ChC) or Árkai index (ÁI) to monitor the reaction's progress.

Twenty-four metamarl samples were collected within the Priabonian and Mesozoic cover formations of the Dauphinois. Sampling was restricted to these formations in order to minimize the petrological effect on the IC. The outcrops density also limited sampling around the Dormillouse and Fournel valleys outcrops are poor. Moreover, westward the Selle Fault cut out the Priabonian formation. The nature, age and tectonic setting of this fault are poorly constrained leading to uncertainties on its effects on the metamorphic pattern. Therefore, samples were taken in the Dormillouse, Fournel, Beassac and Chambran valleys and in the Yret zone (Figs. 1, 2).

In the different samples, the main schistosity is related to the D_1 phase (Trullenque 2005), the D_2 phase only affects the area south of an E-W line of Beassac valley. The clay fraction analysed is generally related to D_1.

Samples with detrital mica visible in hand specimen and/or weathered specimens were avoided as far as possible to eliminate detrital contamination. Mineral abbreviations used are from Kretz (1983).

3.1 X-ray diffraction

Clay mineral separation was conducted using techniques described by Potel et al. (2006). Carbonate removal was done using a 5 % acetic acid ($C_2H_4O_2$) and washed after with deionised water. To minimize the effect of possible detrital clay minerals, we avoided long grinding processes (<15 s) and repeated the settling procedure for the ≤2 µm fraction five times. Illite and chlorite crystallinity was measured at the University of Giessen on air-dried preparates, using a D501 Bruker-AXS (Siemens) diffractometer, Cu$K\alpha$ radiation at 40 kV and 30 mA and divergence slits of 0.5° with a secondary graphite monochromator. Two slices of each sample were prepared and each measured two times as air-dried and one time glycolated. The range of measurement, the time counting and the step size were as follow: for whole-rock paragenesis between 2 and 70 $\Delta°2\Theta$ with 1 s and 0.02° step, for air-dried preparate between 2 and 70 $\Delta°2\Theta$ with 2 s and 0.01° step.

Illite "crystallinity" was calculated using the software DIFFRACPlus (evaluation/release 2001 by ©Bruker AXS) and MacDiff 4.25 (written by R. Petschick, 17 May 2001). IC measured in Giessen ($IC_{Giessen}$) values were transformed into KI values using a correlation with the SW standards (CIS standards) of Warr and Rice (1994) ($KI_{CIS} = 1.2702 \times IC_{Giessen} - 0.0314$) (Table 1). The KI was used to define the limits of anchizone, and the transition values were chosen as follows: KI = 0.25 $\Delta°2\Theta$ for the epizone to high anchizone boundary, KI = 0.30 $\Delta°2\Theta$ for the high to low anchizone boundary and KI = 0.42 $\Delta°2\Theta$ for the low anchizone to diagenetic zone. However, the use of the CIS standards is not universally accepted as giving Kübler-equivalent zone limits. Kisch et al. (2004) show that the CIS standard values are much broader than those obtained by all other laboratories and that the high- and low-grade boundaries of the anchizone of the raw values of Warr and Rice (1994) are much broader than the Kübler-equivalent. This discrepancy is likely to reflect errors in the conversion of the IC values into Kübler equivalent (Kisch et al. 2004; Ferreiro Mählmann and Frey this volume; Ferreiro Mählmann et al. this volume). Therefore, following the recommendations done by Kisch et al. (2004), we published in the Table 1 the $IC_{Giessen}$ and ChC to allow comparison with other laboratories. The same experimental conditions were also used to determine chlorite "crystallinity" on the (002) peak of the second (7 Å) basal reflections of chlorite (Table 1). The ChC measurements were calibrated with those of Warr and Rice (1994) and expressed as the ÁI (Guggenheim et al. 2002): $ÁI = 0.8775 \times ChC + 0.0239$. The anchizone boundaries for the ÁI were defined by correlation with the KI and are given as 0.24 $\Delta°2\Theta$ for the epizone to anchizone boundary and 0.30 $\Delta°2\Theta$ for the anchizone to diagenetic zone.

Randomly oriented samples for K-white mica *b* cell dimension and polytype determination of K-white mica were prepared using wood glue on quartz sample holder. The K-white mica *b* cell dimension is based on the $d_{060,331}$ spacing and on the increasing celadonite substitution that

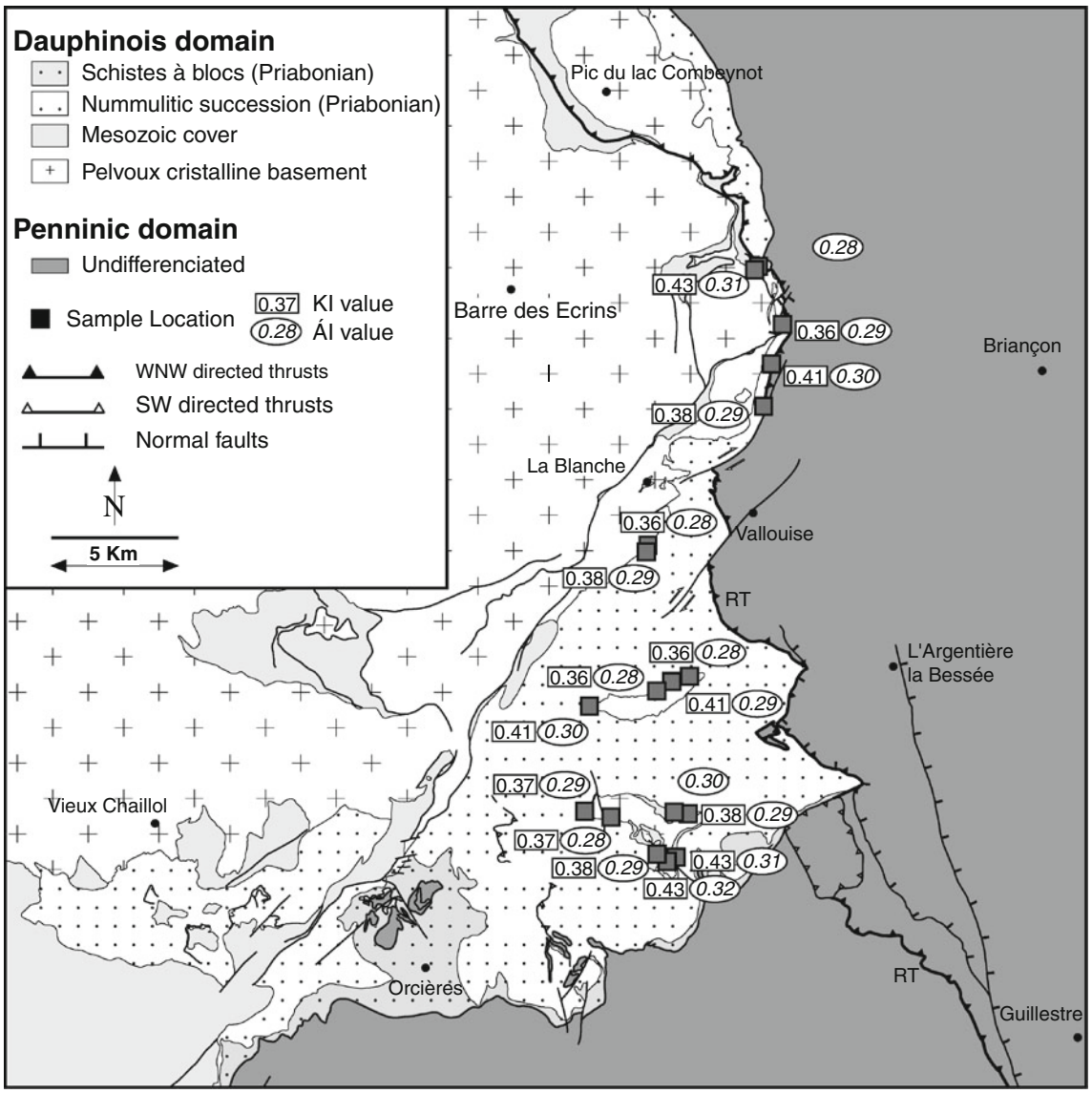

Fig. 2 Distribution and values of Kübler index (KI) and Árkai index (ÁI) in the studied area. Due to the proximity of the samples Do4,4a,4b; Do5a,c; DoF1a,b; Fo1b,c,e; Fo2b,c and Fo3a,b,c the values are shown as averages. *RT* Roselend thrust

occurs with pressure increase in white mica (Ernst 1963; Guidotti et al. 1989). Guidotti et al. (1989) presented linear regression equations that quantify the changes in the K-white mica *b* cell dimensions of muscovite $2M_1$ that result from cation substitutions on the interlayer and octahedral sites. The K-white mica *b* cell dimension value was determined by measurement of the (060) peak of the potassic white mica, if present (Sassi and Scolari 1974), by using the cell-refinement program WIN-METRIC V.3.0.7 (©Bruker AXS).

Illite-muscovite polytype determination was done using a curve of $2M_1/(2M_1 + 1M)$ peaks ratio calibrated using different mixture of illite polytype following the technique described by Dalla Torre et al. (1994). Merriman and Peacor (1999) recognized that the wealth of data on variations in white mica polytypism as a function of temperature is generally consistent with predictable trends. However, they recommended that polytype sequences should not be used other than as indicators of reaction progress.

3.2 Microthermometry

Quartz-calcite veins were sampled along the Rocher de l'Yret shear zone (RYSZ) (Figs. 1, 2), in order to substantiate P–T estimation and to reconstruct the fluid evolution history during metamorphism (Frey et al. 1980). Microthermometry investigations were done at the University of Giessen on double polished thin sections and performed using a Linkam THM 600/S/Geo heating-freezing

Table 1 Samples identification, stratigraphic age, Illite Kübler index and chlorite "crystallinity" values of the <2 μm grain-size fraction samples (data in Δ°2θ), percent of $2M_1$ polytypes and K-white mica *b* cell dimension data

Sample	Sratigraphic age	Elevation (m)	$IC_{Giessen}$ Δ°2Θ	KI Δ°2Θ	1σ Δ°2Θ	ChC Δ°2Θ	ÁI Δ°2Θ	1σ Δ°2Θ	$\%2M_1$	b (Å)
Bea	Priabonian	1,350	0.31	0.36	0.004	0.30	0.28	0.004	92	9.024
Beb	Priabonian	1,370	0.33	0.38	0.004	0.30	0.29	0.007	87	9.009
CHA1	Priabonian	1,700	0.33	0.38	0.007	0.30	0.29	0.008	89	9.008
CHA2	Priabonian	1,710	0.36	0.41	0.004	0.32	0.30	0.010	72	9.015
CHA3	Priabonian	1,720	0.32	0.36	0.002	0.30	0.29	0.008	84	9.001
Do1	Mesozoic Cover	1,500	0.33	0.38	0.001	0.30	0.29	0.005	81	8.998
Do2	Mesozoic Cover	1,520	0.35	0.40	0.002	0.32	0.30	0.010	–	9.006
Do4a	Priabonian	1,835	0.33	0.38	0.004	0.30	0.29	0.012	–	9.026
Do4b	Priabonian	1,835	0.34	0.39	0.006	0.30	0.29	0.013	–	9.025
Do4	Priabonian	1,840	0.30	0.34	0.012	0.29	0.28	0.012	96	9.010
D05a	Mesozoic Cover	2,100	0.33	0.38	0.004	0.31	0.30	0.006	89	9.004
Do5c	Mesozoic Cover	2,105	0.32	0.37	0.008	0.31	0.29	0.010	79	9.007
DoF1a	Mesozoic Cover	1,700	0.35	0.41	0.003	0.32	0.30	0.007	–	–
DoF1b	Mesozoic Cover	1,700	0.38	0.45	0.001	0.33	0.32	0.019	73	–
DoF2	Priabonian	2,400	0.37	0.43	0.001	0.34	0.32	0.021	85	–
DoF3	Priabonian	2,200	0.33	0.38	0.004	0.30	0.29	0.004	84	9.025
Fo1b	Priabonian	1,800	0.32	0.37	0.002	0.30	0.28	0.011	88	9.018
Fo1c	Priabonian	1,740	0.31	0.35	0.004	0.29	0.28	0.021	90	9.010
Fo1e	Priabonian	1,740	0.33	0.38	0.003	0.30	0.28	0.009	–	–
Fo2b	Priabonian	1,760	0.32	0.37	0.001	0.30	0.28	0.005	95	9.017
Fo2c	Priabonian	1,760	0.31	0.36	0.004	0.30	0.29	0.006	90	9.019
Fo3a	Priabonian	2,100	0.31	0.35	0.002	0.29	0.28	0.009	82	9.028
Fo3b	Priabonian	2,100	0.36	0.42	0.004	0.32	0.31	0.007	81	9.025
Fo3c	Priabonian	2,100	0.39	0.46	0.017	0.32	0.31	0.010	70	–
Fo4b	Priabonian	1,640	0.35	0.41	0.004	0.31	0.29	0.005	90	9.016
YR1	Priabonian	2,700	0.37	0.43	0.006	0.33	0.31	0.003	81	9.021
YR2	Priabonian	2,700	0.34	0.39	0.006	0.29	0.28	0.010	–	–

IC illite "crystallinity" measured in Giessen, *KI* Kübler Index, *ChC* chlorite "crystallinity"of the 002 chlorite peak, *AÍ* Árkai Index, $\%2M_1$ percent of $2M_1$ polytypes. *b(Å)* K-white mica *b* cell dimension

stage coupled to a TMS 94 temperature controller with an error of ±1 °C. The stage is mounted on an Olympus microscope with a 100× Objective. The heating and cooling stage was calibrated using synthetic fluid inclusion calibration standard: CO_2 and H_2O from ©Bubbles Incorporation.

Two-phase (consisting of vapour and liquid at room temperature) fluid inclusions were identified. No dissolved volatile phase was observed, either by melting of CO_2 at or below its triple point of −56.6 °C, nor by formation or dissolution of clathrate or liquid–vapor equilibrium of a volatile component such as higher hydrocarbons (HHC), CH_4, CO_2, N_2 or H_2S. Thus, microthermometry was restricted to measuring the melting temperature of ice (Tm_{ice}) and the bulk homogenization temperature of the fluid inclusions (Th_i). As none of the investigated fluid inclusions contained any observable gas component, salinity was derived from the ice melting temperature in NaCl-equivalence after Hall et al. (1988). Density for fluid inclusions with homogenisation temperatures less than 200 °C are from the equations of state given by Brown and Lamb (1989) and for temperatures greater than 200 °C are from Zhang and Frantz (1987). The isochores were calculated from the equation of state given by Zhang and Frantz (1987).

3.3 Raman microspectrometry

Gas, liquid and solid phases were investigated at the University of Frankfurt am Main using a Raman microprobe Leica/Renishaw and the software Renishaw WiRE^{TM} 2.0 and GRAMS. An Argon laser (green laser: $\lambda = 514.5$ nm) was used as excitation laser radiation. The Raman microspectrometry was used to identify the presence of CH_4, CO_2, HHC (C_2H_6 or C_3H_8) and N_2 in fluid inclusions. The relevant peak is positioned at 2,917 cm^{-1} for CH_4, 1,285 and 1,388 cm^{-1} for CO_2, 2,890 and 2,954 cm^{-1} for C_2H_6 or C_3H_8, respectively and 2,331 cm^{-1} for N_2 (Burke 2001). The small size of most fluid inclusions (<10 μm) and the large vertical dimension of the laser beam focus (4 μm in diameter) cause the presence of Raman lines of the

enclosing quartz (1,160 cm^{-1}) in the spectra of fluids. This line does not interfere at all with the CH_4, CO_2 and N_2 lines.

4 Results

4.1 Mineralogy

The mineralogy of the studied samples is given in Table 1.

In the Priabonian and Mesozoic meta-marls, the mineral assemblages consist of quartz + K-white micas + chlorite and calcite with minor amounts of albite. Gypsum is detected in some samples from the Fournel and Dormillouse valleys (Do2, Fo3a and Fo3c). In the fraction <2 μm, illite-muscovite predominates, chlorite and quartz are significant, and feldspar, if detected, is only present in small quantities.

4.2 Characteristics of the phyllosilicates

Figure 2 shows the distribution of the KI data, the values of which are listed in Table 1.

The values in the Dormillouse valley vary between uppermost diagenetic conditions (0.43 Δ°2Θ) in the south and low anchizonal values (0.36 Δ°2Θ) in the north. In the Fournel, Beassac and Chambran Valleys, the KI data indicate low anchizonal conditions (0.35–0.41 Δ°2Θ). In the Yret Zone, illite crystallinity values correspond to the diagenesis/anchizone boundary (0.37–0.43 Δ°2Θ) (Fig. 2). No trend can be observed between KI and elevation of the sample. However, a trend can be observed in each valley or zone, with an increase from south to north of KI values. This is similar to that Aprahamian (1988) described.

The distribution of ÁI values are presented in Fig. 2. The pattern of very low-grade metamorphism shown by AÍ agrees well with the pattern of the KI (Fig. 2). A positive linear correlation ($R^2 = 0.64$) is found between KI and ÁI values (Fig. 3a). This gives confidence on the fact that illite and chlorite "crystallinities" actually refer to the same P–T conditions and thus the same experienced T–t history.

The percentage of $2M_1$ illite-muscovite polytype relative to the KI in the studied area shows a positive trend with increasing metamorphic grade (Fig. 3b).

Sassi and Scolari (1974) determined a semi quantitative relationship between the K-white mica *b* cell dimension and the metamorphic pressure gradient under greenschist facies condition. They plotted the K-white mica *b*-values as cumulative frequency curves in order to compare them with other metamorphic belts. Guidotti and Sassi (1986) collated published K-white mica *b* cell dimension data for greenschist and blueschist facies rocks. They presented a qualitative plot of *b* cell dimension as a family of curves in

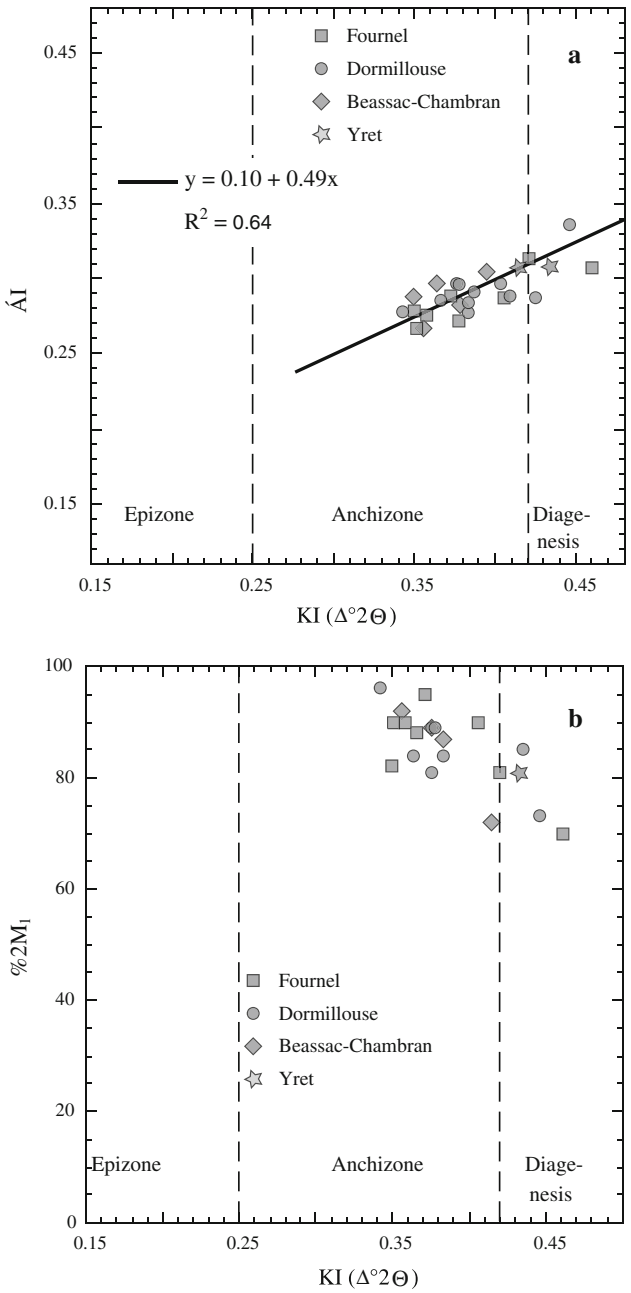

Fig. 3 Correlation between Kübler index (KI) and Árkai index (AÍ) (**a**) and the $2M_1/1M_d$ illite polytype ratio (**b**), all derived from air-dried mounts

P–T space. The values presented by Guidotti and Sassi (1986) do not extend to the sub-greenschist facies. However, the considerable amount of K-white mica *b* cell dimension data from very low-grade metapelites accumulated in different metamorphic belt corroborate the groupings found by Guidotti and Sassi (1986), as shown by Merriman and Peacor (1999). K-white mica *b* cell dimensions were calculated for 21 samples from the anchizone (three samples were not integrated due to interferences and poor intensity signal), all fall in the same range with a

minimum 8.998 and a maximum 9.028 Å values (Table 1). Specimens from the Mesozoic cover have lower values (at around 9.000 Å), while Priabonian are centred around 9.020 Å. However, both value groups are in the intermediate pressure facies (between 9.000 and 9.040 Å) as shown in Fig. 4 (the curve obtained is similar to the reference curve from Ryoke), suggesting an inferred geothermal gradient of 25–35 °C/km (Guidotti and Sassi 1986).

4.3 Vein mineralogy, textural relationships and microthermometry

Samples were collected within the RYSZ, previously decribed by Butler (1992), and consisting in an imbricate of basement slices and para-autochtonous sedimentary cover. This shear zone, lying directly below the frontal penninic nappe stack, has been considered as the map trace of the RT in this area (Trullenque 2005). All kinematic indicators measured in the field or deduced from microfabric analysis of calcite ultramylonites (Trullenque et al. 2006), consistently show a WNW directed sense of transport, consistent with activity along the RT. No evidence of D_2 structures are found in this area.

Samples have been collected along strike slip fault planes dissecting basement slices and indicating a clear WNW directed sense of transport. These faults are clearly related to the first deformation phase D_1. The chronology of the different fluid inclusion populations (Table 2) is a relative one with respect to their host mineral and their overgrowth (Mullis 1976).

Veins are mainly composed of small quartz crystals associated sometimes with calcite crystals. Only two-phase fluid inclusions (consisting of vapour and liquid at room temperature) were identified with the microscope. Fibre quartz is observed in the sample F72. In *F92*, two fluid inclusion assemblages are identified. The first one is a two-phase type in the host quartz and probably of primary type, i.e. trapped during mineral growth. The second one is overprinting the first assemblage and probably of pseudo-secondary type. The true temperature of entrapment of the fluid inclusions, i.e. mineral growth, was constrained by intersecting the isochores of primary two-type phase fluid inclusions with the inferred geothermal gradient deduced from the K-white b cell dimension (Fig. 5). Isochores were calculated for the lower and upper homogenization temperature (Th_i) with an average salinity of 5.6 and 13.8 wt. % NaCl equivalent for samples F72 and F92, respectively.

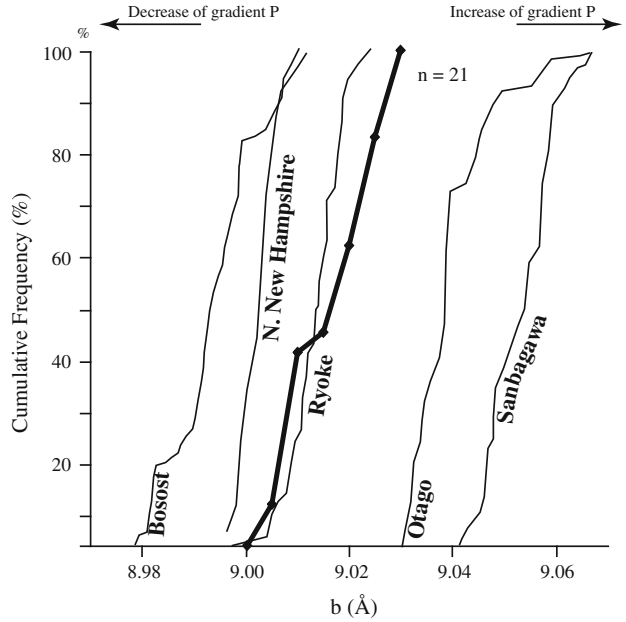

Fig. 4 Cumulative curves of K-white mica *b* cell dimensions for 21 anchizonal samples from our study area (*in bold*) with reference curves from Sassi and Scolari (1974) and Guidotti and Sassi (1986)

5 Discussion

The structural metamorphic map of the Alps (Oberhänsli et al. 2004) indicates lower sub-greenschist facies E of the

Table 2 Fluid inclusion data of two quartz samples from the Yret Zone, Western French Alps

1 Locality	2 FP	3 HM	4 IT	5 n_I	6 V %	7 Tm_{ICE}	8 Th_I	9 H_2O mole %	10 NaCl mole %
F72	1	FQ	P	66	5	−3.5 ± 0.6	176.6 ± 18.3	94.5	5.6
F92	1	VQ	Ps II	22	5	−6.9 ± 0.9	182.4 ± 15.5	89.8	10.2
“	2	VQ	P	3	5–10	−9.6 ± 0.9	172.3 ± 10.0	87.2	13.8

(1) Locality number. (2) *FP* fluid inclusion population. (3) *HM* host mineral—*FQ* fibre quartz, *VQ* vein quartz. (4) *IT* inclusion type—*Ps II* pseudosecondary fluid inclusions, *P* primary fluid inclusions. (5) n_I number of measured fluid inclusions. (6) *V* % volume % of the volatile part estimated at room temperature. (7) Tm_{Ice} melting temperature of ice (°C)—First number = mean value, second number = standard deviation. (8) Th_I homogenization temperature of fluid inclusions—First number = mean value, second number = standard deviation. (9) and (10) = approximate mole-% H_2O and NaCl (equivalents)

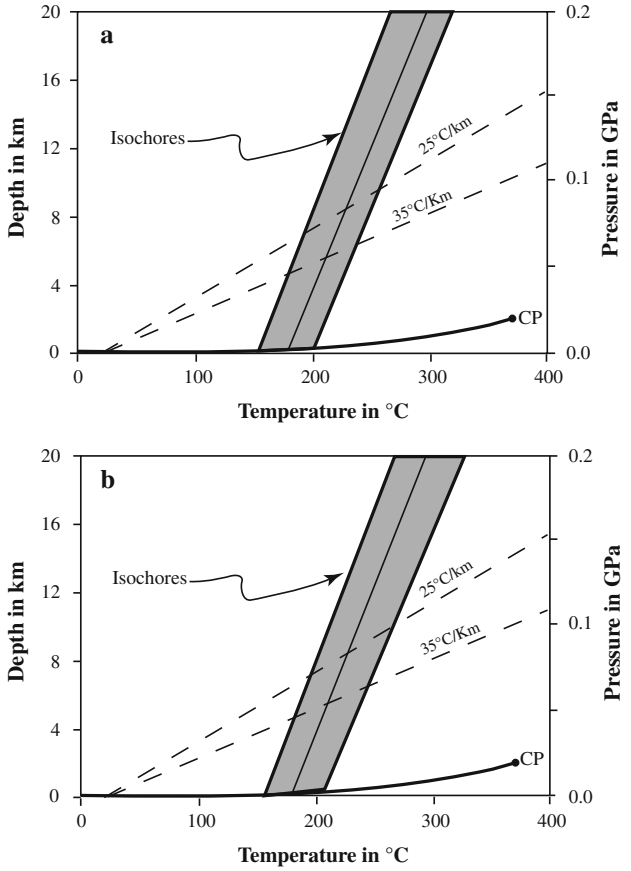

Fig. 5 Depth-temperature diagrams with isochores representing the higher and the lower calculated molar volumes for vapour-rich fluid inclusions and the meam isochores in samples F72 (**a**) and F92 (**b**) from the Yret zone. The *dashed lines* represent the range of geothermal gradients from 25 and 35 °C/km as deduced from the K-white mica b cell dimensions. The *thick curve* represents the liquid–gas reaction curve of water. *CP* critical point of water

RT and N of the Pelvoux massif. North of the Pelvoux massif, Ceriani et al. (2003) described an E–W metamorphic gradient on the E side of the RT. In the Briançonnais, they reported an increase from anchizonal to epizonal conditions from E to W. In the same area, the Dauphinois domain (in the footwall of the RT) shows epizonal metamorphic conditions. The Dauphinois domain in this area is only affected by one deformation phase, corresponding to the third deformation phase in the FPU (Ceriani 2001; Ceriani et al. 2001) and equivalent to D_1 in our studied area (Trullenque 2005). The K-white *b* cell dimensions obtained by Ceriani et al. (2003) in the Dauphinois Domain are ranging between 9.000 and 9.030 Å similar to those obtained in our study, indicating similar geothermal metamorphic gradient between the two areas.

Frey (1987) and Essene and Peacor (1995) showed that KI cannot be used as a precise geothermometer and only provide an approximate temperature range. In spite of this, attempts have been made to relate KI values to absolute temperatures. This was done in different low-grade metamorphic units by comparing the KI data with other geothermometers (Ferreiro Mählmann 1994, 1996; Merriman and Peacor 1999; Mullis et al. 2002; Potel et al. 2006). Mullis et al. (2002) have suggested a diagenesis—anchizone boundary in the Alps on the basis of a comparison of IC versus FI data. This allows to better define the range of temperature that the SE of the Pelvoux massif was subjected during tectonic evolution.

The KI values indicate that the Dauphinois domain in the SE of the Pelvoux massif underwent up to low anchizonal metamorphic conditions (Table 1; Fig. 2). According to Mullis et al. (2002), the boundary is linked to a temperature of around 230–240 °C (similar to the compilation results from Ferreiro Mählmann (1994)). This can be compared to the temperature estimates obtained west of our studied area in the "grès de Champsaur" (W of Prapic). Waibel (1990) described quartz–prehnite ± calcite veins in the "grès de Champsaur". The country rock is dark green in colour, enriched in pumpellyite of variable composition, and to a lesser extent prehnite, at the expense of laumontite. Aprahamian (1988) described also mottled sandstone (faciès moucheté), the pale-coloured mottles being enriched in laumontite as cement and as partial replacement product of albitized clastic plagioclase and the darker areas being relatively enriched in chlorite cement. According to Frey et al. (1991) and Potel et al. (2002), the coexistence of zeolites (laumontite in this case) and prehnite–pumpellyite is restricted to a rather small P–T area below 240 °C and therefore in the range obtained by using the correlation from Mullis et al. (2002).

Zircon FT data were gained from the turbiditic "grès de Champsaur" and the underlying Pelvoux crystalline basement (Seward et al. 1999). These data provide important information on the peak temperatures reached during Alpine metamorphism. For the zircon FT system, several estimates on the temperature range of the partial annealing zone exist (e.g. Yamada et al. 1995, 2007; Tagami et al. 1998). Tagami et al. (1998) suggested a temperature range between 200 and 320 °C to be appropriate, which covers the temperature range relevant to the metamorphic zonation based on illite "crystallinity" (e.g. Mullis et al. 2002). The combination of both methods therefore provides additional constraints on the maximum temperature reached to the SE of the Pelvoux massif. In the Glarus Alps, the comparison between fluid inclusion data and zircon FT data suggests that zircon FT annealing in the Taveyanne sandstone (a lateral equivalent of the "grès de Champsaur") only becomes detectable above 250 °C (Rahn 2001). The measured K-white mica *b* cell dimension values inferred an intermediate geothermal gradient with 25–35 °C/km (Merriman and Peacor 1999). This gradient seems to be a very conservative approach, however the

result is similar to that found in the Dauphinois domain north of the Pelvoux massif (Ceriani et al. 2003). Combining this information with the fluid inclusion data obtained in the Yret zone, a trapping temperature for the fluid inclusions of 220 ± 10 °C can be obtained (Fig. 5a, b). Consequently, the comparison of KI, FT and fluid inclusion leads to the conclusion that the SE of the Pelvoux massif was subjected to temperatures higher than 200 °C, but lower than 250 °C. This is higher than the estimation of temperature by Seward et al. (1999) who estimated that the burial temperature of the "grès de Champsaur" was not higher than 200 °C. This implies metamorphic burial between 7 and 9 km. Neither our KI nor the FT data (Seward et al. 1999) reveal the presence of a metamorphic gradient from E to W in the SE of the Pelvoux massif as described by Aprahamian (1974). The absence of epizonal KI values in the Vallouise valley (Aprahamian 1974, 1988), moves the anchizone–epizone boundary to the N of the Pelvoux massif, where epizonal metamorphic conditions are observed (Ceriani et al. 2003). As mentioned by Ferreiro Mählmann and Frey (2012), one of the reasons of the lack of epizonal values, is that the KI values obtained by CIS calibration led to a broadening of the anchizone area.

The available metamorphic data from the south of the Pelvoux massif combined with the available deformation data allow us to deduce some conclusions concerning the tectono-metamorphic evolution in this area. A first important result provided by the KI, fluid inclusion and FT data is the fact that the Dauphinois domain exhibits lower metamorphic conditions compared to the Penninic domain. According to the metamorphic map of the Alps, the Penninic domain west of the RT is metamorphosed under lower greenschist facies (Oberhänsli et al. 2004). Field evidences SE of the Pelvoux massif (this paper; Trullenque 2005), indicate that D_1 corresponds to the first penetrative schistosity, marked by very fine-grained K-white mica, chlorite, quartz and albite. The metamorphic gradient observed and the formation of the fluid inclusions studied are related to this deformation phase and the burial heating (with a maximum of 9 km burial) was generated by the overthrusted Penninic domain along the RT onto the Dauphinois domain. As mentioned above, the K-white mica *b* cell dimension values in our studied area SE of the Pelvoux massif, are similar to those obtained in the north by Ceriani et al. (2003). Therefore, the metamorphic gradient observed in the Penninic domain must be established before D_1, as observed by Ceriani et al. (2003) further to the N (the D_1 observed SE of the Pelvoux massif correspond to the D_3, see above). So, we have no trace of an older metamorphic event.

North of the Pelvoux massif, the metamorphic grade is higher with epizonal conditions and may be explained by thicker Penninic units on top of the Dauphinois domain leading to higher degree of burial and therefore show a regional metamorphic gradient increasing from S to N. This is corroborated by the same pressure gradient observed north and south of the Pelvoux massif in the Dauphinois domain (same range of K-white mica *b* cell dimension).

Ferreiro Mählmann (2001) in the eastern Alps showed that in rocks submitted to a long metamorphic event (20 Ma) and a steady state heat flow, the smectite content in the anchizone is between 0 and 5 % (90 % of the samples without smectite), and that under stabile thermal conditions (equilibrium), KI can be used as a thermometer. In this region, Henrichs (1993) reported K-white mica *b* cell dimension values between 9.000 and 9.022 Å and the compilation of the Ferreiro Mählmann et al. (2012) shows a normal to low geothermal gradient (30 °C/km). Comparison of our results with KI and K-white mica *b* cell dimension values will suggest that the Dauphinois Domain has been submitted to a relative long heating time like in the eastern Alps.

6 Conclusion

The tectono-metamorphic history of the Dauphinois domain in the SE of the Pelvoux is similar that described by Ceriani et al. (2003) in the north. Peak metamorphic conditions in the Dauphinois domain are reached during the overthrusting of the Penninic units during D_1 top-WNW directed thrusting along the RT. The metamorphism is characterized by temperatures below 250 °C and higher than 200 °C and a metamorphic gradient between 25 and 35 °C, and a long time event. This range of temperature is compatible with the FT data published by Seward et al. (1999) indicating that the burial temperature in the region was lower than 250 °C. Based on our KI values and the mineral paragenese observed in the W of the "grès de Champsaur", no E–W metamorphic zonation as described by Aprahamian (1974, 1988) is observed. But, in the studied area, the grade of metamorphism in the Dauphinois Domain is lower than in the northern of the Pelvoux massif (Ceriani et al. 2003) confirming the N–S metamorphic zonation described by Aprahamian (1974, 1988). This is also outlined by the zircon FT ages indicating an increase in age primarily from the north to the south (Fügenschuh and Schmid 2003) and supports their hypothesis that the more southerly located areas were lees deeply buried and hence less exhumed. Like proposed by Ceriani et al. (2001) and Fügenschuh and Schmid (2003), the overthrust along the RT of the Penninic units may caused burial and metamorphism in the external Dauphinois units.

Acknowledgments This manuscript benefited greatly from constructive and helpful reviews and comments from M. Rahn and R. Ferreiro Mählmann.

References

Apps, G. M., Peel, F., & Elliott, T. (2004). The structural setting and palaeogeographical evolution of the Gres d'Annot Basin. Deep-water sedimentation in the Alpine Basin of SE France; new perspectives on the Gres d'Annot and related systems. *Geological Society Special Publication, 221*, 65–96.

Aprahamian, J. (1974). La cristallinité de l'illite et les minéraux argileux en bordure des massifs cristallins externes de Belledonne et du Pelvoux. *Géologie Alpine, 50*, 5–15.

Aprahamian, J. (1988). Cartographie du métamorphisme faible à très faible dans les Alpes françaises externs par l'utilisation de la cristallinité de l'illite. *Geodinamica Acta, 2*, 25–32.

Árkai, P. (1991). Chlorite crystallinity: an empirical approach and correlation with illite crystallinity, coal rank and mineral facies as exemplified by Palaeozoic and Mesozoic rocks of northeast Hungary. *Journal of Metamorphic Geology, 9*, 723–734.

Árkai, P., Faryad, S. W., Vidal, O., & Balogh, K. (2003). Very low-grade metamorphism of sedimentary rocks of the Meliata unit, Western Carpathians, Slovakia: implications of phyllosilicate characteristics. *International Journal of Earth Sciences, 92*, 68–85.

Árkai, P., Sassi, F. P., & Sassi, R. (1995). Simultaneous measurements of chlorite and illite crystallinity: a more reliable tool for monitoring low- to very low grade metamorphism in metapelites. A case study from the Southern Alps (NE Italy). *European Journal Mineralogy, 7*, 1115–1128.

Brown, P. E., & Lamb, W. M. (1989). P-V-T properties of fluids in the system $H_2O \pm CO_2 \pm NaCl$: new graphical presentations and implications for fluid inclusion studies. *Geochimica Cosmochimica Acta, 53*, 1209–1221.

Bürgisser, J. (1998). *Deformation in foreland basins of the Western Alps (Pelvoux massif, SE France); significance for the development of the Alpine arc*. Zürich: ETH. 151 pp.

Burke, E. A. J. (2001). Raman microspectrometry of fluid inclusions. *Lithos, 55*, 139–158.

Butler, R. W. H. (1989). The influence of pre-existing basin structure on thrust system evolution in Western Alps. *Geological Society Special Publications, 44*, 105–122.

Butler, R. W. H. (1992). Thrust zone kinematics in a basement-cover imbricate stack; eastern Pelvoux massif, French Alps. *Journal of Structural Geology, 14*, 29–40.

Ceriani, S. (2001). A combined study of structure and metamorphism in the frontal Penninic units between the Arc and the Isère valleys (Western Alps): Implications for the geodynamics evolution of the Western Alps. Unpublished PhD thesis, Universität Basel, 196 pp.

Ceriani, S., Fügenschuh, B., Potel, S., & Schmid, S. M. (2003). The tectono-metamorphic evolution of the Frontal Penninic units of the Western Alps: correlation between low-grade metamorphism and tectonic phases. *Schweizerische Mineralogische und Petrographische Mitteilungen, 83*, 111–131.

Ceriani, S., Fügenschuh, B., & Schmid, S. M. (2001). Multi-stage thrusting at the "Penninic Front" in the Western Alps between Mont Blanc and Pelvoux massifs. *International Journal of Earth Sciences, 90*, 685–702.

Coward, M. P., Gillcrist, R., & Trudgill, B. (1991). Extensional structures and their tectonic inversion in the Western Alps. *Geological Society Special Publications, 5*, 93–112.

Dalla Torre, M., Stern, W. B., & Frey, M. (1994). Determination of white K-mica polytype ratios: comparaison of different XRD methods. *Clay Minerals, 29*, 717–726.

Davies, V. M. (1982). Interaction of thrusts and basement faults in the French external Alps. *Tectonophysics, 88*, 325–331.

Debrand-Passard, S., Courbouleix, S. & Lienhardt, M.-J. (1984). Synthèse géologique du Sud-Est de la France. Mémoire du Bureau de recherches géologiques et minières, 126 pp.

Desmons, J., Compagnoni, R. & Cortesogno, L. (1999). Alpine metamorphism of the Western Alps: II. High-P/T and related pre-greenschist metamorphism. In: Frey, M., Desmons, J. & Neubauer, F. (Eds.), *The new metamorphic map of the Alps. Schweizerische Mineralogische und Petrographische Mitteilungen*, *79* (pp. 111–134).

Ernst, W. G. (1963). Significance of phengitic micas from low grade schists. *American Mineralogist, 48*, 1357–1373.

Essene, E. J., & Peacor, D. R. (1995). Clay mineral thermometry—a critical perspective. *Clays Clay Mineral, 43*, 540–553.

Ferreiro Mählmann, R. (1994). Zur Bestimmung von Diagenesehöhe und beginnender Metamorphose-Temperaturgeschichte und Tektogenese des Austroalpins und Süpenninikums in Vorarlberg und Mittelbünden. Universität Frankfurt, *Frankfurter Geowissenschaftliche Arbeiten, Serie C 14*, 498 pp.

Ferreiro Mählmann, R. (1996). The pattern of diagenesis and metamorphism by vitrinite reflectance and illite-"crystallinity" in Mittelbünden and in the Oberhalbstein. Part2: correlation of coal petrographical and of mineralogical parameters. *Schweizerische Mineralogische und Petrographische Mitteilungen, 76*, 23–46.

Ferreiro Mählmann, R. (2001). Correlation of very low-grade data to calibrate a thermal maturity model in a nappe tectonic setting, a case study from the Alps. *Tectonophysics, 334*, 1–33.

Ferreiro Mählmann, R., Bozkaya, O., Potel, S., Le Bayon, R., Šegvić, B. & Nieto García, F. (2012). The pioneer work of Bernard Kübler and Martin Frey in very low-grad metamorphic terranes: Paleo-geothermal potential of Kübler-Index/organic matter reflectance correlation – a review. *Swiss Journal of Geosciences*, this volume.

Ferreiro Mählmann, R. & Frey, M. (2012). **"**Standardisation, calibration and correlation of the Kübler-Index and the vitrinite/bituminite reflectance: an inter-laboratory and field related study". *Swiss Journal of Geosciences*, this volume.

Frey, M. (Ed.). (1987). *Low temperature metamorphism*. Glasgow and London: Blackie & Son.

Frey, M., de Capitani, C., & Liou, J. G. (1991). A new petrogenetic grid for low-grade metabasites. *Journal of Metamorphic Geology, 9*, 497–509.

Frey, M., Desmons, J. & Neubauer, F. (Eds.) (1999). The new metamorphic map of the Alps. *Schweizerische Mineralogische und Petrographische Mitteilungen, 79*, 230 pp.

Frey, M., Teichmüller, M., Teichmüller, R., Mullis, J., Künzi, B., Breitschmid, A., et al. (1980). Very low-grade metamorphism in external parts of the Central Alps: illite crystallinity, coal rank and fluid inclusion data. *Eclogae Geologicae Helvetiae, 73*, 173–203.

Fügenschuh, B., & Schmid, S. (2003). Late stages of deformation and exhumation of an orogen constrained by fission-track data: a case study in the Western Alps. *Geological Society of America Bulletin, 115*, 1425–1440.

Fügenschuh, B., Loprieno, A., Ceriani, S., & Schmid, S. M. (1999). Structural analysis of the Subbrian çonnais and Valais units in the area of Mo ûtiers (Savoy, Western Alps): paleogeographic and tectonic consequences. *International Journal of Earth Sciences, 88*, 201–218.

Gillcrist, R., Coward, M., & Mugnier, J. L. (1987). Structural inversion and its controls; examples from the Alpine Foreland and the French Alps. *Geodinamica Acta, 1*, 5–34.

Guggenheim, S, Jr, Bain, D. C., Bergaya, F., Brigatti, M. F., Drits, V. A., Eberl, D. D., et al. (2002). Report of the association internationale pour l'étude des argiles (AIPEA) nomenclature committee for 2001: order, disorder and crystallinity in phyllosilicates and the use of the 'crystallinity index'. *Clays and Clay Minerals, 50*, 406–409.

Guidotti, C. V., & Sassi, F. P. (1986). Classification and correlation of Metamorphic Facies Series by Means of Muscovite b_0 data from Low-Grade Metapelites. *Neues Jarbuch Mineralogie Abteilunghefte, 153*, 363–380.

Guidotti, C. V., Sassi, F. P., & Blencoe, J. G. (1989). Compositional controls on the a and b cell dimensions of $2M_1$ Muscovites. *European Journal of Mineralogy, 1*, 71–84.

Gupta, S. (1997). Tectonic control on paleovalley incision at the distal margin of the early Tertiary Alpine foreland basin, southeastern France. *Journal of Sedimentary Research, 67*, 1030–1043.

Hall, D. L., Sterner, S. M., & Bodnar, R. J. (1988). Freezing point depression of NaCl–KCl–H_2O solutions. *Economic Geology, 83*, 197–202.

Henrichs, C. (1993). Sedimentpetrographische Untersuchungen zur Hochdiagenese in der Kössen-Formation (Ober Trias) der westlichen Ostalpen und angrenzenden Südalpengebiete. *Bochumer geologische und geo-technische Arbeiten 40*, 206 pp.

Huyghe, P., & Mugnier, J. L. (1995). A comparison of inverted basins of the southern North Sea and inverted structures of the external Alps. *Geological Society Special Publications, 88*, 339–353.

Kisch, H. J., Árkai, P., & Brime, C. (2004). On the calibration of illite Kübler index (illite 'crystallinity'). *Schweizerische Mineralogische und Petrographische Mitteilungen, 84*, 323–331.

Kretz, R. (1983). Symbols for rock-forming minerals. *American Mineralogist, 68*, 277–279.

Kübler, B. (1964). Les argiles, indicateurs de métamorphisme. *Institut Français Pétrole, 19*, 1093–1112.

Kübler, B. (1968). Evaluation quantitative du métamorphisme par la cristallinité de l'illite. Etat des progrès réalisés ces dernières années. *Bulletin Centre Recherche Pau, S.N.P.A., 2*, 385–397.

Lazarre, J., Tricart, P., Courrioux, G., & Ledru, P. (1996). Héritage téthysien et polyphasage alpin; réinterprétation tectonique du "synclinal" de l'aiguille de Morges (massif du Pelvoux, Alpes occidentales, France). *Comptes Rendus de l'Académie des Sciences, Série II. Sciences de la Terre et des Planètes, 323*, 1051–1058.

Merriman, R. J., & Peacor, D. R. (1999). Very low-grade metapelites: mineralogy, microfabrics and measuring reaction progress. In M. Frey & D. Robinson (Eds.), *Low-Grade Metamorphism* (pp. 10–60). London: Blackwell Science.

Merriman, R. J., Roberts, B., & Peacor, D. R. (1990). A transmission electron microscope study of white mica crystallite size distribution in a mudstone to slate transitional sequence, North Wales, U. *K. Contributions to Mineralogy & Petrology, 106*, 27–40.

Mullis, J. (1976). Das Wachstumsmilieu der Quarzkristalle im Val d'Illiez (Wallis, Schweiz). *Schweizerische Mineralogische und Petrographische Mitteilungen, 56*, 219–268.

Mullis, J. J., Rahn, M. K. W., Schwer, P., de Capitani, C., Stern, W. B., & Frey, M. (2002). Correlation of fluid inclusion temperatures with illite "crystallinity" data and clay mineral chemistry in sedimentary rocks from the external part of the Central Alps. *Schweizerische Mineralogische und Petrographische Mitteilungen, 82*, 325–340.

Oberhänsli, R., Bousquet, R., Engi, M., Goffé, B., Gosso, G., Handy, M., Höck, V., Koller, F., Lardeaux, J.-M., Polino, R., Rossi, P., Schuster, R., Schwarz, S. & Spalla, M.I. (2004). Metamorphic structure of the Alps (1:1'000'000), Commission for the Geological Map of the World (UNSECO), Paris.

Perriaux, J., & Uselle, J. P. (1968). Quelques données sur la sédimentologie des grès du Champsaur (Hautes-Alpes). *Géologie Alpine, 44*, 329–332.

Potel, S., Ferreiro, Mählmann R., Stern, W. B., Mullis, J., & Frey, M. (2006). Very low-grade metamorphic evolution of pelitic rocks under high-pressure/low-temperature conditions, NW New Caledonia (SW Pacific). *Journal of Petrology, 47*, 991–1015.

Potel, S., Schmidt, S Th, & de Capitani, C. (2002). Composition of pumpellyite, epidote and chlorite from New Caledonia—How important are metamorphic grade and whole-rock composition? *Schweizerische Mineralogische und Petrographische Mitteilungen, 82*, 229–252.

Rahn, M. K. W. (2001). *The metamorphic and exhumation history of the Helvetic Alps, Switzerland, as revealed by apatite and zircon fission tracks. Unpublished Habilitation thesis*. Freiburg: Albert-Ludwigs-Universität. 140 pp.

Ravenne, C., Vially, R., Riche, P., & Tremolieres, P. (1987). Sédimentation et tectonique dans le bassin marin Eocene supérieur-Oligocene des Alpes du Sud. *Revue de l'Institut Français du Pétrole, 42*, 529–553.

Sassi, F. P., & Scolari, A. (1974). The b_0 of the potassic white micas as a barometric indicator in low-grade metamorphism of pelitic schists. *Contributions to Mineralogy and Petrology, 45*, 143–152.

Schmid, S. M., Fügenschuh, B., Kissling, E., & Schuster, R. (2004). Tectonic map and overall architecture of the Alpine orogen. *Eclogae Geologicae Helvetiae, 97*, 93–117.

Seward, D., Ford, M., Bürgisser, J., Lickorish, H., Williams, E. A., & Meckel, L. D, I. I. I. (1999). Preliminary report on fission tracks studies in the Pelvoux area, SE France. *Memorie di Scienze Geologiche, 51*, 25–31.

Sue, C., Tricart, P., Dumont, T., & Pecher, A. (1997). Raccourcissement polyphase dans le massif du Pelvoux (Alpes occidentales): exemple du chevauchement de socle de Villard- Notre-Dame. Comptes Rendus de l'Académie des Sciences, Série II. *Sciences de la Terre et des Planètes, 324*, 847–854.

Tagami, T., Galbraith, R. F., Yamada, R. & Laslett, G. M. (1998). Revised annealing kinetics of fission tracks in zircon and geological implications. In P. Van den haute, & F. De Corte (Eds.), Advances in fission-track geochronology: Kluwer academic publishers, Dordrecht, The Netherlands, pp 99–112.

Tricart, P. (1986). Le Chevauchement de la zone briançonnaise au Sud-Est du Pelvoux; clé des rapports zone externe—zones internes dans les Alpes occidentales. *Bulletin de la Societé Géologique de France, Huitième Série, 2*, 233–244.

Tricart, P. (2004). From extension to transpression during the final exhumation of the Pelvoux and Argentera massifs, Western Alps. *Eclogae Geologicae Helvetiae, 97*, 429–439.

Tricart, P., Bourbon, M., Chenet, P. Y., Cros, P., Delorme, M., Dumont, T., et al. (1988). Tectonique synsédimentaire triasico-jurassique et rifting téthysien dans la nappe briançonnaise de Peyre-Haute (Alpes occidentales). *Bulletin de la Societé Géologique de France, 4*, 669–680.

Tricart, P., Schwartz, S., Sue, C., Poupeau, G., & Lardeaux, J. M. (2001). La dénudation tectonique de la zone Ultradauphinoise et l'inversion du front Briançonnais au Sud Est du Pelvoux (Alpes Occidentales); une dynamique Miocène á actuelle. *Bulletin de la Societé Géologique de France, 172*, 49–58.

Trullenque, G. (2005). Tectonic and microfabric studies along the Penninic Front between Pelvoux and Argentera Massifs (Western Alps, France). Unpublished PhD thesis, Universität Basel, 301 pp.

Trullenque, G., Kunze, K., Heilbronner, R., Stünitz, H., & Schmid, S. (2006). Microfabrics of calcite ultramylonites as records of

coaxial and non-coaxial deformation kinematics: examples from the Rocher de l'Yret shear zone (Western Alps). *Tectonophysics, 424*, 69–97.

Waibel, A.F. (1990). Sedimentology, petrographic variability, and very-low-grade metamorphism of the Champsaur sandstone (Paleogene, Hautes-Alpes, France). Evolution of volcaniclastic foreland turbidites in the external Western Alps. Unpublished PhD thesis, Université de Genève, 140 pp.

Warr, L. N., & Rice, A. H. (1994). Interlaboratory standardization and calibration of clay mineral crystallinity and crystallite size data. *Journal of Metamorphic Geology, 12*, 141–152.

Yamada, R., Galbraith, R. F., Murakami, M., & Tagami, T. (2007). Statistical modelling of annealing kinetics of fission-tracks in zircon; reassessment of laboratory experiments. *Chemical Geology, 236*, 75–91.

Yamada, R., Tagami, T., Nishimura, S., & Ito, H. (1995). Annealing kinetics of fission tracks in zircon: an experimental study. *Chemical Geology (Isotope Geoscience Section), 122*, 249–258.

Zhang, Y., & Frantz, J. D. (1987). Determination of the homogenization temperatures and densities of supercritical fluids in the system NaCl-KCl-CaCl2-H2O using synthetic fluid inclusions. *Chemical Geology, 64*, 335–350.